Blur-Invariant Copy-Move Forgery Detection Technique with Improved Detection Accuracy utilising SWT-SVD

SK.AYESHA (M.Tech scholar)[1]
R SUDHEER BABU MTech, (Ph.D.) (Asst Professor)[2]
Electronics and communication Engineering Department [1,2]
G. PULLAREDDY College of Engineering and Technology, Andhra Pradesh-518007,India[1,2]
ayeshashaik404@gmail.com[1]

ABSTRACT

In this paper we are detecting the copy-move forgery by using the stationary wavelet transform (SWT). In the previous there are so many algorithms came which operates on the principle of image block matching. When the edges of the forced regions are in the blur state then the detection of forgery will becomes complicate. Here by using SWT we are reducing that problem. SWT is having different properties compared to the DWT like shift invariant. So by using the SWT the noise in between the blocks and it is also helpful to find the similarities i.e. matches and dissimilarities. Using the value decomposition (SVD) we can obtain the blocks, in that blocks features are extracted. To reduce the invariance blur the color-based segmentation is used. In the results of the proposed method we can see the efficiency in the process of detection of copy-move forgery involving intelligent edge blurring. Compared with previous methods SWT is given the better experimental results.

Key points: SWT, SVD, DWT, Colour based segmentation, Blur invariance

I. INTRODUCTION

In today's cyber world, the easy availability of highly advanced equipment and technology, and their wide accessibility to every common man, has put the credibility of digital data highly at stake. Today, neither a charge card number, nor a government disability number, not in any case a financial balance number can be utilized as a confirmation, sufficiently reliable to affirm one's personality.

Advanced pictures, being the real data transporters in the present computerized world, go about as the essential wellsprings of confirmation towards any occasion in the official courtroom and media and communicate enterprises. In any case, the relative straightforwardness of altering and controlling advanced pictures have made their legitimacy and dependability to a great extent faulty. Truth be told, seeing is no all the more accepting, because of the way that in the present computerized age, there is a growing number of malevolently adjusted pictures.

Using a broad assortment of compelling programming applications, advanced picture controls by an enemy have turned out to be to a great degree normal and basic. This can be a basic task when images are utilised as fundamental proof to impact judgment, for instance, in the court of law. Digital Forensics involves the use of logical techniques towards the examination, investigation and understanding of confirmations Derived from computerized hotspots for the thought process of encouraging the remaking of occasions, thusly it is bolstered ill-conceived antagonistic exercises.

Digital image forensics deals with analysis of image contents for investigation and detection of forgeries to an image. In this work, we address the inconvenience of identifying duplicate move fraud or locale duplication assault [1– 10], That is one of the most extreme crude and also general sorts of digital picture forgeries, wherein the forger copies region(s) of an photograph and pastes it onto itself at some other location(s), with the malicious target to obscure or repeat significant image object(s). The nearness of homogeneous surface in characteristic pictures,

which incorporates water, sky, grass, sand, foliage et cetera make everything of the more noteworthy at risk to this state of assault.

A case of this ambush is approved in Fig. 1. The discovery of copy stream imitation or locale duplication in an photograph is made extra tough by using an intelligent adversary, through blurring of edges of the solid region, in order that traditional pixel block matching algorithms fail to discover the forgery. In this paper, we advise a copy-move forgery detection set of rules which is robust to facet blurring of the duplicate region(s).

Majority of the prevailing area duplication detection strategies are block based totally [4, 5], i.E. They aim to discover pixel blocks which are exact continuous copies of every different in an image. Such methods are effective in detection of copy-move forgery, where an image region is duplicated without any form of alteration to it. However, for region duplication that involves region transformations such as scaling, rotation, edge blurring and so on, such block-based methods do not prove to be equally efficient. In this case, the Key-point-based algorithms are substantially beneficial. Unlike the block-primarily based algorithms, key-point based algorithm totally depends on reproduction-circulate forgery detection strategies [11, 12] rely upon the identification and selection of excessive entropy photograph regions, called the key points. However, although these algorithms are robust against image transformations, they suffer from relatively high computational complexity. Our commitment in this paper is change of a Forensic method for obscure invariant copy pass fraud identification in advanced pix.

Fig. 1 Copy-move forgery:

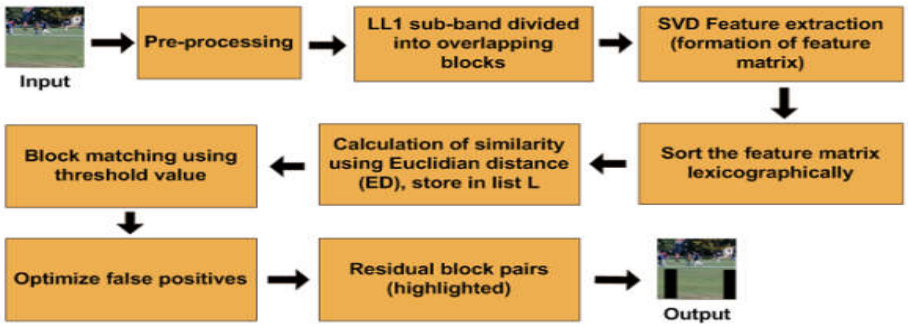

Fig. 2 Operational flowchart

The proposed approach decays a picture into its recurrence sub-groups utilizing table beyond any doubt wavelet rebuild (SWT) [13], and extricates abilities from the SWT sub-groups utilizing solitary rate deterioration (SVD) [14].The shift invariance, un decimated characteristics of SWT, and occasional computational complexity and balance of SVD, makes the Proposed method considerably green in comparison with the contemporary [1–10].

Also, in the proposed technique, we introduce the idea of computerized threshold becoming to optimise manual attempt. Colour-based segmentation [15] has been used in these paintings to obtain blur invariance. Further, to reduce the large variety of false positives produced while an photo includes tremendous regions of homogeneous texture, we have used a eight-connected community checking [15]. The relaxation of the paper is organized as follows. A overview of the cutting-edge is offered in Section 2. Section 3 provides the proposed method for detection of simple replica-pass forgery, in element. The proposed obscure invariant duplicate stream falsification recognition strategy has been provided in Section 4. Our test impacts are displayed in Section five. At long last, we complete in Section 6.

II .RELATED WORK

In one of the pioneer researches in this area, Fridrich et al. [2] proposed region duplication detection based on the principles of exact block matching, autocorrelation, exhaustive block search and robust match [based on discrete cosine transform (DCT)]. The robust matching method proves to be most efficient, where the detection is based on matching of quantisation DCT coefficients, lexicographically sorted for computation efficiency. However, this method, when applied to images containing large identical textured regions, leads to a ton of false matches. Farid and Popescu [4] showed a computationally successful copy move extortion acknowledgment procedure in light of crucial part examination (PCA).

Here, the inborn dimensionality decrease qualities of PCA have been utilized to diminish the quantity of highlights to half of that of [2]. Be that as it may, due to dimensionality reduction, the efficiency reduces for lossy compressed or rotated images. Kang and Wei [5] proposed a place duplication detection technique based on SVD, which is extremely powerful in instances of replica regions prompted with noise. Zhang et al. [6] proposed an algorithm primarily based on discrete wavelet rework (DWT) for replica-flow forgery detection, which once more attains a substantially Low computational complexity in evaluation with the opportunity present schemes.

A sorted neighbourhood approach primarily based on DWT and SVD has been proposed by Li et al. [10], wherein first DWT is connected to the photograph after which SVD is utilized to separate the highlights of the squares of the low-recurrence parts, principle to estimation markdown of the squares. Yang et al. [7] connected un annihilated move invariant dyadic wavelet improve (DyWT) on a fashioned photo by utilizing breaking down it into 4 recurrence subbands, and highlight deteriorated low-recurrence subband into covering squares. The Euclidean separation among each square combine is processed and the coordinating sets are identified the use of a limit. This method optimizes the number of false matches, even when image consists of extensive uniform regions. Another DyWT-based approach, capable of detecting lossy compressed duplicate image regions, where both low- as well as high-frequency components are utilised to get rid of false positives, is proposed by Muhammad et al. [9]. Bayram et al. [8] proposed a Fourier Mellin transform based method, using Bloom filters. This approach turns out to be scale and pivot invariant and additionally computationally effective, having the capacity to recognize fabrication even in shockingly packed previews.

Mahdian and Saic proposed an obscure minute invariant approach for uncovered pics, corrupted through obscuring or clamor. The greater part of the above strategies be afflicted by fake positives and are vulnerable to blurring. In this paper, we endorse a blur-invariant area duplication detection technique with decreased fake effective charge (FPR) and advanced detection accuracy (DA).

III .PROPOSED SWT-SVD BASED COPY-MOVE FORGERY DETECTION

In this area, we talk in detail the activity of the proposed approach for duplicate move falsification discovery, without obscuring of the strong district. A square chart speaking to the operational buoy of the proposed technique Is tested in Fig. 2. In the accompanying subsections we study in detail the responsibilities of the proposed approach.

3.1 Pre-processing

The pre-processing step includes two operations. First, if the probably forged input photograph is a color one, it's miles transformed from RGB to grayscale [15], the usage of the subsequent method:

$$I = 0.299R + 0.587G + 0.114B \quad (1)$$

Second, SWT [13] is implemented to the enter grey scale photo to obtain 4 subbands, viz. Approximation (LL), horizontal (LH), vertical (HL) and diagonal or detail (HH), particularly denoted as LL1, LH1, HL1 and HH1, respectively, at scale 1. In the proposed approach, we use SWT due to the following inherent residences [20, 21] of it over conventional transforms as DWT. (i) The inherent translation invariant belongings of SWT makes it a ideally fitted technique for detection of reproduction-moved photograph quantities. Due to this belongings, even if a sign is shifted, its SWT coefficients do not change. DWT does now not keep shift invariance. In replica-flow forgery, the duplicate regions aren't always placed in the same (relative) pixel positions of two blocks. If the descriptors vary with translation, they result into different representations, corresponding to these two blocks, and

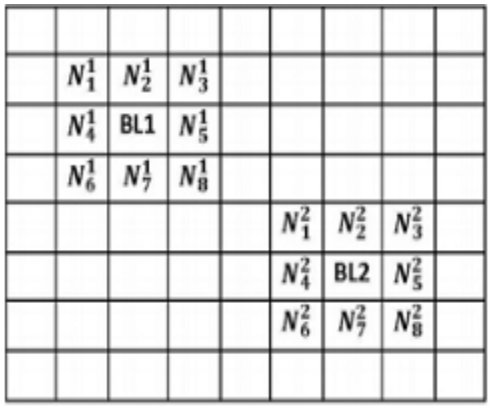

Fig.3 8-connected neighbours of blocks BL1 and BL2

Hence lead to incorrect inference by the region duplication detection algorithm. Since SWT is translation invariant, in such situations the descriptors are NOT altered, hence producing maximum accuracy in copy-move forgery detection. (ii) SWT performs efficient area detection, because of which it allows green detection of blurring along the rims of duplicated place(s). (iii) SWT is relevant to discrete (photo) signals of any arbitrary size. (On the opposite, DWT is suitable simplest for images having dimensions in powers of two.)

3.2 Feature Extraction using SVD:

The LL1 subband that gives the smoothed rendition of the picture, say of size M × N pixels, is apportioned into covering squares of size B × B pixels, which is thought to be littler than the Span of the synthetic area to be outstanding, for this reason giving an combination quantity of M − B + 1 × N − B + 1 squares. However, to reap a

good DA, the block length must not be too small either. The more we growth the block length, the greater features we acquire and the better accuracy we will expect. Experimental results referring to the variation of DA with unit forgery detection block length, has been offered in Section five. SVD [14] is implemented to every block to extract its corresponding singular values characteristic vectors. In the proposed technique, SVD feature extraction proves to be effective, because of the following properties [2–4]:

(i) SVD is considerably less computationally intensive and stable technique which is invariant to translation.

(ii) The dimension of the image matrices need not be fixed for SVD. The matrix can be square as well as rectangular.

(iii) The effectiveness of the SVD gives a natural arithmetical properties of a picture.

(iv) Singular vectors compare to the geometrical qualities (estimate, shape, position and so forth.) of articles inside a picture.

3.3 Sorting of Image Blocks

The feature vectors of the blocks that are stored row-wise in a matrix, called the feature matrix, resulting in a total number of

M − B + 1 × N − B + 1 rows, are lexicographically sorted each.

3.4 Calculation of Similarity

The Euclidean distance D(u, v) between a pair of rows (blocks), say u and v, where u = u1, u2, . . . , ur and v = v1, v2, . . . , vr is computed by D u,

$$D(u,v) = \left(\sum_{i=1}^{r}(u_i, v_i)^2\right)^{1/2} \quad (2)$$

provided blocks u and v are not more distant than a offset threshold, say T f, that signifies the maximum number of rows to compare, i.e. abs index u − index v ≤ T f. This helps to select only those similar blocks which can be expected to have been copy-moved. There is no need to find the Euclidean distance of all the block pairs, but only the very similar blocks that are side by side to each pixel (as specified by T f), in the lexicographically sorted feature matrix, thus decreasing the computation time. The computed Euclidean distance values, along with their corresponding block pairs, are stored in a list L.

3.5 Block Matching using Threshold

The list L now consists of all the square combines that are to be additionally prepared for identification of fraud. The length of L relies upon the span of the picture, the square size and furthermore the counterbalance edge T f. L can be long if the picture is huge, the square size is little or T f is high. Hence, now L requires to be truncated appropriately so as to hold the relatively more similar block pairs than the rest. Thus, a similarity threshold Td, that helps to filter out less similar blocks from the list L, keeping block pairs having a greater probability to have been duplicated, is fitted. An automatic threshold fitting approach, followed in the proposed algorithm, has been discussed in Section 3.7. All the rows in L whose Euclidean distances are more than the similarity threshold Td are discarded, as they are considered to be non-duplicated parts of the images. Further verification is performed on the rest of the pairs that pass this stage of elimination, as follows. For a given block pair, say block1 with coordinates i, j and block 2 with coordinates k, l , the offset of coordinates between block 1 and block2 is given by C

$$C_{12} = \max[abs(i-k), abs(j-l)] \quad (3)$$

Block 1 and block2 are labelled as suspected duplicated regions if C 12 ≥ Ts where Ts is the minimum separation between duplicated regions. All such blocks that pass this filter are detected to be duplicated by the proposed method.

3.6 Optimising False Matches

During copy-move forgery detection, when an image is comprised of extensive regular textured regions, such as blue sky, green grass or scenery with a lot of greenery all around, a sandy desert or beach and so on, conventional copy-move forgery detection algorithms tend to produce huge FPR. This is due to the fact that in such cases, large parts of the image are naturally similar, and hence lead to incorrect detection results. To solve this problem, we adopt 8-connected neighborhood checking [15]. Here, all the blocks that are detected to be duplicates are marked, and considered. For each marked block, its 8-connected neighbours, i.e. up, down, left, right and the four diagonals (as shown in Fig. 3), are checked. The number of neighbours that were also detected as duplicates by above subsection are counted. If this count is > x (some empirical value ≥ 1 and ≤ 7, say 4), then the original block is kept marked. Else, if the count is ≤ x, the original block is considered to be a false positive and hence unmarked.

All the residual marked blocks are output as duplicated or forged. Now the number of false positives has been optimised. After block matching step, it is observed that false matches arise due to similarities in region of uniform natural or textured image. According to our experimental outcomes in Section 5, during reproduction-pass forgery detection in standard test images, initially the FPR varied between 1.17 and 4.63%, which was reduced 0.43 to 2.16% by proposed 8-connected neighbourhood checking.

3.7 Threshold Fitting

Here, we present the detailed threshold fitting technique adopted in Algorithm 1. Manual threshold fitting: Threshold fitting is a crucial step in the proposed copy-move forgery detection algorithm. The threshold may be viewed as a barrier between the authentic and forged regions of the image. Hence, it requires utmost care while being chosen. A perfect fit may be obtained empirically, through selection of various random thresholds (in the valid range), then running the algorithm iteratively for all, and finally selecting the one that produces the most accurate forgery detection results. However, this naive process involves intense computational complexity and constant human interactions. Also, this threshold would vary from image to image. So in this paper we are introducing the concept of automatic threshold fitting as discussed next.

The Institution of Engineering and Technology 2017 303 Automatic threshold fitting: In the proposed algorithm (according to Section 3.5),by this we can say that the threshold values the list of block pairs into two parts. Empirical studies suggest that the part of L satisfying the threshold condition is only 0.1 − 0.3% of the entire list. This is our key observation, That is used as a piece of this paper to get the imagined feature suit along these lines. Once-over L is masterminded in rising solicitation to procure list Lsort, and a while later the point of confinement regard is been the Euclidean division of the rectangular incorporate this is discovered some place close to 0.001 and zero.003th position of the sorted out once-over. The feature is enrolled as

$$T_d = ED_{sort_1} \times N \times 0.001; \quad (4)$$

where ED sort_1 is the Euclidean distance of the topmost block pair in sorted list L sort, and N is the total number of entities presented in L. Next, we present an example calculation of threshold Td values for a particular 256 × 256 test image, and the corresponding false match results, as shown in

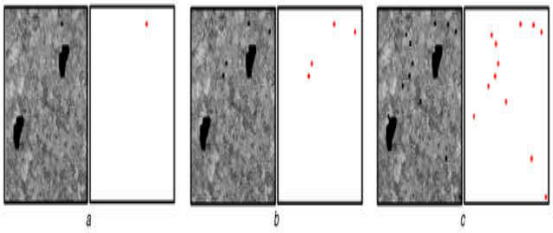

Fig. 4. The procedure for threshold calculation in the proposed algorithm is given in Algorithm 1 (Automatic_Threshold_Fitting).

Algorithm 1: Automated_Threshold_Fitting

1: **Input**: list (L) storing Euclidian distances of block pairs, N are the length of L;
2: **Output**: Threshold Td;
3: $L \leftarrow [ED_1, ED_2, \dots ED_N]^T$;
4: $L_{sort} \leftarrow [ED_{sort\_1}, ED_{sort\_2}, \dots, ED_{sort\_N}]^T \leftarrow Sort_{Assending}(L)$;
5: $\boldsymbol{for}\ i = 1,2, \dots, N\ \boldsymbol{do}$
6: $T_{d_i} \leftarrow \left[ED_{sort_i} \times N \times 0.001\right]$;
7: $\boldsymbol{end\ for}$
8:$T \leftarrow [T_{d_1}, T_{d_2}, T_{d_3}, \dots, T_{d_N}]^T$; $/* For\ demonstrating\ example */$
9: $T_d \leftarrow Td_1$; $/* Actual\ threshold\ adopted */$
10: $Return\ T_{d_1}$;

Example: For the image shown in Fig. 4, the list L is obtained (according to the process described in Section 3.1–Section 3.5), and stored in an ascending order in list Lsort,which is

$$L_{sort} = \begin{bmatrix} 0.0899 \\ 0.1102 \\ 0.1187 \\ 0.1231 \\ 0.1307 \\ \vdots \end{bmatrix}$$

Depending on the Lsort entries, we populate the list T according to Algorithm 1 (Automated _Threshold_Fitting), as

$$T = \begin{bmatrix} 0.0899 \times 40520 \times .001 = 3.64 \\ 0.1102 \times 40520 \times .001 = 4.46 \\ 0.1187 \times 40520 \times .001 = 4.81 \\ 0.1231 \times 40520 \times .001 = 4.98 \\ 0.1307 \times 40520 \times .001 = 5.29 \\ \vdots \end{bmatrix}$$

The false matches corresponding to the first, third and fifth entries in T are shown in Fig. 4. It is evident from Fig. 4 that the least value of T d gives the lowest FPR. In our work, the first entry in list T is adopted as the threshold Td.

IV. BLUR-INVARIANT COPY-MOVE FORGERY DETECTION

Many times, an intelligent adversary blurs a region of an image in the process of duplication, specifically its edges, so as to ensure that it does not stand out or seem out of place due to the abrupt variations along the edges. This makes the image imperceptible to human eyes, In addition to helps to keep away from detection of the forgery via traditional replica-move forgery detection algorithms along with [2, 4–6].

In this segment, we talk the proposed technique for achieving blur invariance in copy-move forgery detection. Blurring any part of an image generates a noise in that area, different from the image's original noise, which is nothing but the undesired variation of colour information or brightness in the image, produced while capturing the image due to electronic noise, and is different from the manual noise caused during blurring the forged part. The diagonal subband (HH) of an image obtained by applying SWT to it Lets in the area of clamor prompted because of obscuring. Key thought applied: The proposed misrepresentation disclosure methodology makes use of pieces of facts for perceiving copy move fake. They are I. Comparability amongst repeated and moved areas within the clean adjustment of a photograph. Ii. Confusion abnormality among the darkened vicinity(s) and anything is left of the bit of the photograph. In Fig.5, we taken a square outline to delineate the operational buoy of the proposed obscure invariant duplicate course phony location. In the accompanying sub-areas, we talk about in component the stairs of the proposed strategy.

4.1 Pre-processing

If the probably cast input photograph is a coloration one, it's miles first transformed to grayscale [9], using (1). Next, SWT [13] is implemented to the input grayscale photo to obtain 4 sub bands, viz. Approximation (LL1), horizontal (LH1), vertical (HL1) and diagonal or detail (HH1), at scale 1.

4.2 Color-Based Segmentation for Blur Invariance

Colour-based segmentation is performed on the image in the L ∗ a ∗ b colour space, using K-means clustering. Segmentation is performed only when blurring is involved in the forgery. This is because, when a forged image involves blurring, the naturally homogeneous textures present in the image exhibit more similarity as compared with the copy-blurred-moved regions. However, this is not true for non-blurred forged images, since here, the copymoved parts are exact copies of each other. It was observed many Fig. 4 False positive results using first, third and fifth thresholds in list T 304 times that the fitted threshold is not able to take care of the false positives caused after blurring; hence this adversely affects the DA of the scheme.

To solve this problem, colour-based segmentation is applied. The image is segmented into, say n segments according to its colours, and the individual segments are handled independently. The individual segments are divided into overlapping blocks of fixed size and then threshold fitting is carried out on each of them.

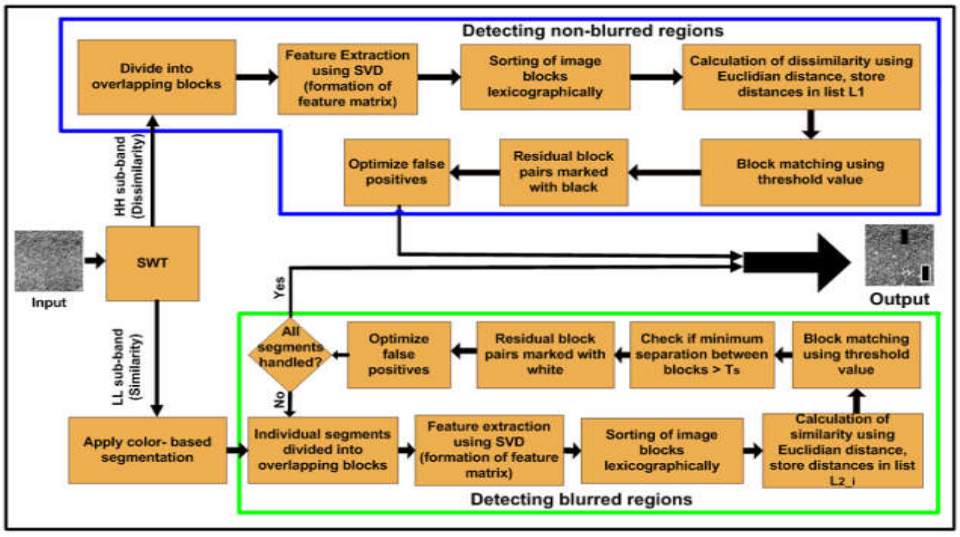

Fig. 5 Operational flowchart

Fig. 6 K-means clustering applied to Lena test image

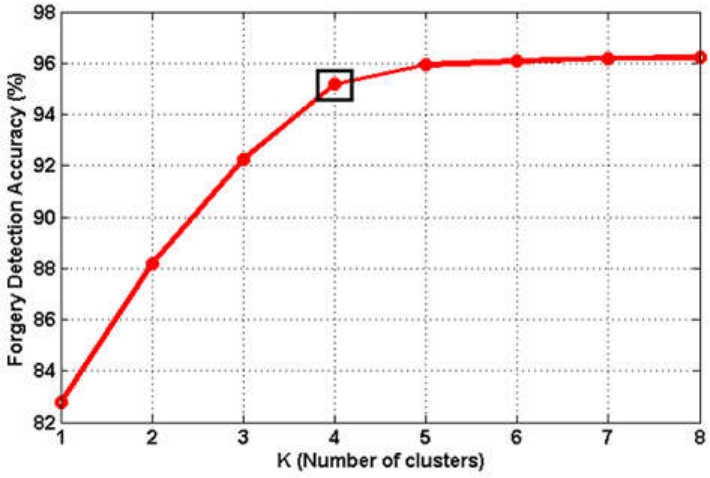

Fig. 7 Elbow method for deciding K

However, now it is done for each individual segment, and not the entire image as a whole. To achieve colour-based Division utilizing K-technique grouping [5], we first change over a photo to its L∗a∗b shading space. The L∗a∗b shading space is picked since it molds the human visual contraption uncommonly proficiently. Likewise, this shading territory being a perceptually uniform symmetrical Cartesian organize contraption is reasonable for this issue. The L∗a∗b∗ space consists of a luminosity layer 'L∗', chromaticity layers 'a∗' and 'b∗', which indicate where a colour lies along the red–green and blue–yellow axes, respectively.

K-means clustering involves two parameters, viz., the number of clusters to be formed, and a distance metric to quantify the degree of closeness of two objects. Here, objects are nothing but the pixels represented by 'a∗' and 'b∗' values. The aftereffect of K-implies grouping is applied to call the pixels. Each institution gets a listing as returned by the K-implies bunching calculation, and every pixel in the photo is marked with its organization list recognized with the aid of diverse grey-scale esteems. The aftereffects of K-implies bunching linked to the Lena photograph, has been shown in Fig. 6. Decision of K:

The value of K is decided by using Elbow method [6]. As we increase K, computational complexity increases. So we select the value of K (number of clusters) in such a way that is further adding cluster causes negligible improvement in forgery DA (for mathematical formulation of DA and other performance parameters, the reader may please refer to Section 5.1). Table 1 presents the correlation between interval in number of clusters and corresponding improvement of DA. In Fig. 7, we have shown the improvement in DA with increase in K. We

observed that after the interval $K \in 4-5$, we obtain negligible improvement of DA by increasing K. In this work, we selected K = 4 following the Elbow method. The results for different values of K, i.e. K = 2, 3, …, 6, in terms of blur invariance, are shown in Fig. 8, for one test image.

4.3 Feature Extraction using SVD

The HH1 subband that captures the details of the image is partitioned into overlapping blocks. In practice, the region undergoing blur is considerably smaller compared with the entire image. Hence, the chosen unit block size should be considerably smaller compared with the image size. However, using extremely small unit blocks (say 2×2) hinders the process by increasing the computation time. So, a correct tradeoff has to be arrived at. Next, the LL1 sub band of the image is divided into overlapping blocks, not for the entire image, but segment-wise. Note here that, segmentation is required for the LL sub band only, not the HH sub band. This is because, segmentation is required here to avoid false positives while finding similarity (using LL); specifically, false positives caused due to blurring visa-vis natural similarities between image regions. However, the HH sub band helps in noise detection, and hence used for recording dissimilarities among image regions. So, segmentation is not required here. Features of each block in HH1 and LL1 (for each segment) are extracted using SVD.

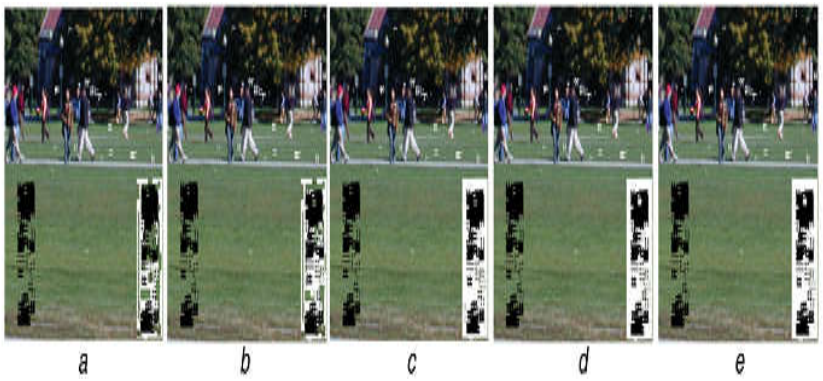

Fig. 8 Blur invariance achieved with K = 2, 3, …, 6 for a single test image

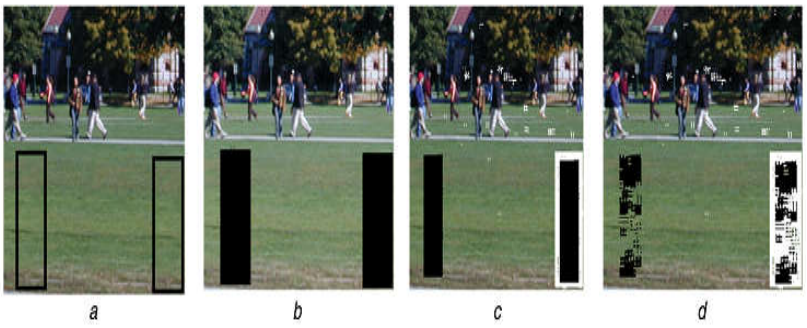

Fig. 9 Copy-move forgery detection results of the proposed method, with and without blurring (a) Manually forged input image, (b) Output obtained when there is no blurring involved, (c) Output obtained when there is blurring along the edges, (d) Output obtained when there is blurring along the edges as well as inside the forged area

4.4 Sorting of Image Blocks

The feature vectors of the blocks are stored row-wise in a matrix, called the feature matrix, and are sorted lexicographically. This is done for blocks of the entire image (HH1) and of each segment too (LL1).

4.5 Calculation of Similarity and Dissimilarity using Euclidean Distance

The Euclidean distances between the pixel values of each pair of blocks in HH1 and LL1 are computed, provided the blocks are as far from each other as possible, the offset threshold say T f h and T f l signifying the maximum number of rows to compare. This is done to get the most dissimilar and most similar blocks that can be expected to have been blurred and possibly copy-moved, respectively. The computed Euclidean distances, along with their corresponding block pairs, are stored into lists L1 and L2_i, where i = 1, 2, …, n and n is the total number of segments.

Table 1 Improvement of DA with K

Interval of *K* values	DA improvement, %
1–2	5.41
2–3	4.08
3–4	2.91
4–5	0.77
5–6	0.14
6–7	0.10
7–8	0.04

4.6 Block Matching using Threshold

A dissimilarity threshold Tdh that helps to filter out less dissimilar block pairs from list L1, keeping block pairs having higher probability of being blurred, is fitted using automatic threshold fitting. Similarly, similarity threshold Tdl_i that helps to filter out less similar blocks of segment i from the list L2_i, keeping block pairs having higher probability of having been duplicated, is fitted. All rows in L1 whose Euclidean distance is less than the dissimilarity threshold Tdh are discarded. Similarly, all rows in L2_i whose Euclidean distances are more than the similarity threshold T dl_i are discarded. Further verification is performed to the rest of the block pairs that pass this stage of elimination. Two blocks, say block1 and block2 are output as duplicates, if the separation between them is ≥ Ts, where Ts is the minimum allowed separation between duplicated regions. This is carried out only for LL1 blocks, not HH1. If two blocks are too close to each other, specifically overlapping, then their feature vectors would also be very similar. Hence, the value of Ts depends on the block size. All such LL1 blocks, for each segment, that pass the above filter are marked in black in the output image. The residual block pairs in L2 are marked white in the output image.

4.7 Optimising False Matches

For both the blackened and whitened blocks, the 8-connected neighbourhood check Is done to discard the false positives as examined in Section 3.6. At last, the following photograph is shown with copy squares appeared in dark, and white squares demonstrating the obscured parts. Note ideal here that, as a result of the shading based absolutely division embraced inside the proposed system, the greater part of the squares are not as looked at any more noteworthy; least difficult intra-segment correlations are executed. The execution of the proposed system as far as copymove fraud recognition, with and without obscuring stressed, has been offered in Fig. Nine. This figure shows a natural image with extensive green (grass) patch, from which a portion has been copymoved manually. In

Fig. 9a, we have shown the forged image. The copy-move forgery detection results using the proposed SWT with SVD based method, for the manually forged input image, have been shown in Figs. 9b–d. Fig. 9b is the output obtained when there is no blurring at all, Fig. 9c is the detection result obtained when the edges of the duplicated region have been blurred and Fig. 9d is the result obtained when there is blurring along the edges as well as in the inner parts of the forged region.

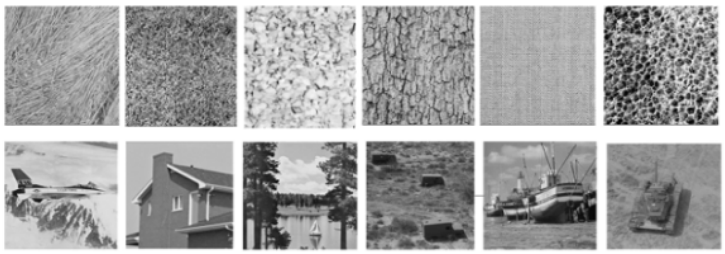

Fig. 10 256 × 256 standard greyscale (texture and natural) test images

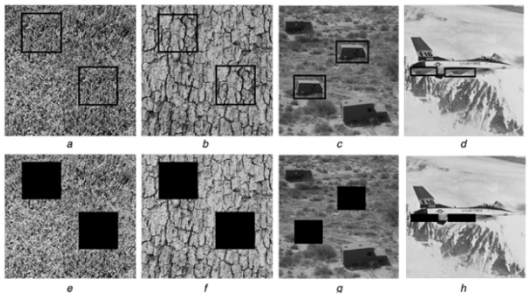

Fig. 11 Manually forged test images with no blurring and corresponding forgery detection results using the proposed SWT–SVD method (a)–(d) Manually induced forgeries, (e)–(h) Duplicate regions detected

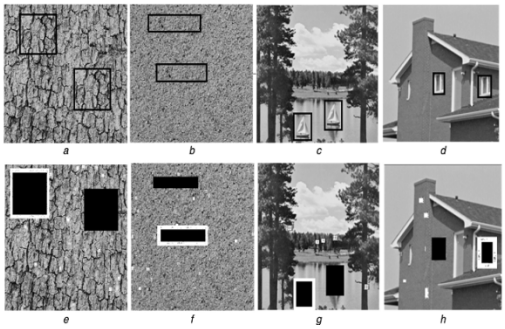

FIG : 12 Manually forged test images with blurring and corresponding forgery detection results using the proposed SWT-SVD method (a)–(d) Manually induced forgeries, (e)–(h) Duplicate regions detected.

V. EXPERIMENTAL RESULTS AND DISCUSSION

The proposed methods were carried out in MATLAB the use of the MATLAB Image Processing Toolbox. Our experiments had been done on 12 widespread 256 × 256 check pictures, along with texture photographs and natural photographs, proven in Fig. 10. In order to avoid experimental bias, all effects offered on this paper are taken as the average over a couple of take a look at pictures of Fig. 10. The overall performance outcomes of the proposed technique, for randomly decided on texture and herbal take a look at snap shots (from Fig. 10) have been shown in Figs. Eleven and 12, for non-blurred and blurred forgeries, respectively.

5.1 Performance Evaluation

For quantitative evaluation of the performance efficiency of the proposed method, we have used DA, defined as

$$DA = \frac{Number\ of\ correctly\ detected\ copy - movied\ pixels}{Number\ of\ pixels\ actually\ copy - moved} \times 100\% \qquad (5)$$

In order to evaluate the performance of the proposed method without blurring, we have varied the unit detection block size, well as the forgery size, and measured the corresponding DA results. These effects had been supplied in Table 2, and are the common effects for all our check snap shots proven in Fig. 10. The DA outcomes of the proposed method when blurring is involved inside the forgery have been shown in Table 3for varying block and forgery sizes. Here, the block sizes for both HH and LL subbands are equal. The results presented in Table 3 represent the average DA over all our test images. Here the evaluation has been done by combining the results obtained by considering both LL (similarities) and HH (noise) subbands.

5.2 Comparison with State-of-the-Art

In this section, we compare the proposed method with state-of-theart in terms of DA. We have varied the forgery size from 10 to 40% in steps of 10%. The outcomes (arrived at the midpoint of over our whole test set) have been introduced in Table 4, which demonstrate that the proposed strategy is impressively more effective as contrasted and the condition of-theart. We likewise show the outcomes in type of two-dimensional plots in Fig. 13.

5.3 Improved False Positives

In this section, we present our experimental results pertaining to usefulness of the 8-connected neighbourhood check with respect to reduction of the FPR. These results have been presented in Tables 5 and 6, for forged images without blurring and with blurring, respectively. FPR is defined as the total number of authentic image pixels, falsely detected to be forged, as

$$FPR = \frac{Number\ of\ pixels\ falsely\ dtetcted\ to\ be\ copy - moved}{Number\ of\ pixels\ actually\ copy - moved} \times 100 \qquad (6)$$

Fig 5.1 Input Forgery Image

Fig 5.2 Segmented Blocks

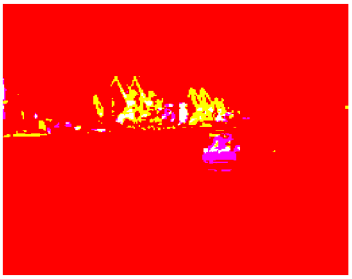

Fig 5.3 LAB Color Transform Image

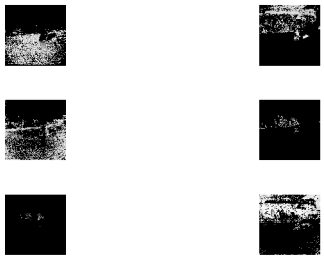

Fig 5.4 Processing On Image to Get

Suspected Region

Fig 5.5 Suspected Region

Fig Detected Regions

Fig 5.6 Forgery Region

Fig 5.7 Forgery Region

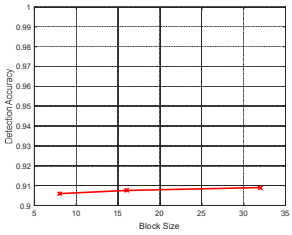

Fig 5.8 Detection of Accuracy

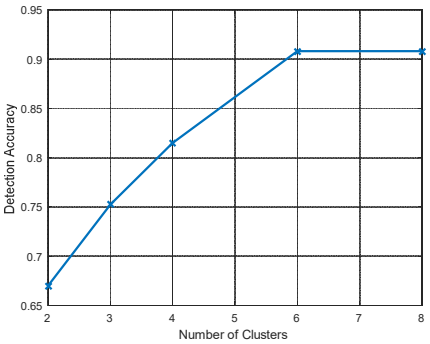

Fig 5.9 Number of Clusters and Block Accuracy

VI.CONCLUSION

In this paper we are proposing a block based copy-move forgery detection based on the SWT with SVD. To reduce the person's involvement and computation time automatic threshold fitting is introduced. Color-based segmentation is used to reduce the blur invariance and to conclude the number of false positives and 8-connected neighborhood checking is also used. In the proposed method the main three stages where we are finding the forgery is copy-move forgery (i) without blurring, (ii) with blurring. Compared to the previous methods we are getting the higher forgery DA. In the future the implementation can be done based on the of image region transformations, such as rotation, rescale and reflection, in copy-move forgery.

REFERENCES

[1] Christlein, V., Riess, C., Jordan, J., et al.: 'An assessment of general copymove adulteration recognizable proof strategies', IEEE Trans. Inf. Wrongdoing scene inquire about Sec., 2012, 6, pp. 1841– 1854

[2] Fridrich, A.J., Soukal, B.D., Luk, A.J.: 'Area of engendering circle creation in virtual pictures'. Proc. Of Digital Forensic Research Workshop, 2003

[3] Huang, Y., Lu, W., Sun, W., et al.: 'Upgraded DCT-based locale of copymove adulteration in sneak peaks', Forensic Sci. Int., 2011, 206, (1), pp. 178– 184

[4] Farid, A.P., Popescu, A.C.: 'Revealing programmed misrepresentations with the manual of spotting duplicated picture region'. Specific Report, Hanover, Department of Computer Science, Dartmouth College, USA, 2004 [5] Kang, X., Wei, S.:

[6] Zhang, J., Feng, Z., Su, Y.: 'another approach for recognizing copy pass creation in virtual pictures'. Eleventh IEEE Singapore Int. Conf. On Communication Systems, 2008, pp. 362– 366

[7] Yang, J., Ran, P., Tan, J.: 'Mechanized photograph creation lawful offense sciences with the guide of procedure for the use of undecimated dyadic wavelet change and zernike minutes', J. Comput. Inf. Syst., 2013, 9, (sixteen), pp. 6399– 6408

[8] Bayram, S., Sencar, H.T., Memon, T.N.: 'A green and tough approach for making sense of reproduction pass creation'. IEEE Int. Conf. On Acoustics, Speech and Signal Processing, 2009, pp. 1053– 1056

[9] Muhammad, G., Hussain, M., Bebisi, G.: 'Reserved reproduction sidestep photograph fake personality using undecimated dyadic wavelet redesign', Digit. Contribute., 2012, 9, (1), pp. Forty 9– fifty seven

[10] Li, G., Wu, Q., Tu, D., et al.: 'A composed system gadget for recognizing replicated districts in picture fakes amass quite gentle of DWT and SVD'. IEEE Int. Conf. On Multimedia and Expo, 2007, pp. 1750– 1753

[11] Huang, H., Guo, W., Zhang, Y.: 'Area of copy pass adulteration in mechanized photos using SIFT computation', Comput. Intell. Ind. Appl., 2008, 2, pp. 272– 276

[12] Bo, X., Junwen, W., Guangjie, L., et al.: 'Picture copy sidestep fake prominence gather really with perceive to SURF'. Int. Conf. On Multimedia Information Networking and Security, 2010, pp. 889– 892

[13] Ilea, D., Whelan, P.: 'The work area bound wavelet revamp and different quantifiable bundles'. Address Notes in Statistics, New York, 1995